

Actin bundling by dynamin 2 and cortactin is implicated in cell migration by stabilizing filopodia in human non-small cell lung carcinoma cells

HIROSHI YAMADA^{1,3}, TETSUYA TAKEDA^{1,3}, HIROYUKI MICHIEUE²,
TADASHI ABE^{1,3} and KOHJI TAKEI^{1,3}

Departments of ¹Neuroscience and ²Physiology, Graduate School of Medicine, Dentistry and Pharmaceutical Sciences, Okayama University; ³CREST, Japan Science and Technology Agency, Kita-ku, Okayama 700-8558, Japan

Received April 6, 2016; Accepted May 25, 2016

DOI: 10.3892/ijo.2016.3592

Abstract. The endocytic protein dynamin participates in the formation of actin-based membrane protrusions such as podosomes, pseudopodia, and invadopodia, which facilitate cancer cell migration, invasion, and metastasis. However, the role of dynamin in the formation of actin-based membrane protrusions at the leading edge of cancer cells is unclear. In this study, we demonstrate that the ubiquitously expressed dynamin 2 isoform facilitates cell migration by stabilizing F-actin bundles in filopodia of the lung cancer cell line H1299. Pharmacological inhibition of dynamin 2 decreased cell migration and filopodial formation. Furthermore, dynamin 2 and cortactin mostly colocalized along F-actin bundles in filopodia of serum-stimulated H1299 cells by immunofluorescent and immunoelectron microscopy. Knockdown of dynamin 2 or cortactin inhibited the formation of filopodia in serum-stimulated H1299 cells, concomitant with a loss of F-actin bundles. Expression of wild-type cortactin rescued the punctate-like localization of dynamin 2 and filopodial formation. The incubation of dynamin 2 and cortactin with F-actin induced the formation of long and thick actin bundles, with these proteins colocalizing at F-actin bundles. A depolymerization assay revealed that dynamin 2 and cortactin increased the stability of F-actin bundles. These results indicate that dynamin 2 and cortactin participate in cell migration by stabilizing F-actin bundles in filopodia. Taken together, these findings suggest that dynamin might be a possible molecular target for anticancer therapy.

Introduction

Cancer cell migration, invasion, and metastasis are preceded by the formation of pseudopodia such as lamellipodia and filopodia. During these cellular processes, F-actin filaments remodel into a higher order structure and then assemble an intricate cytoskeletal network within cells (1). These dynamic three-dimensional changes are mediated by several actin-bundling and crosslinking proteins, and are essential for supporting filopodia at the leading edge of migrating cells (2).

Dynamin plays an essential role in endocytosis, participating in the membrane fission process (3-5). Dynamin also functions in the formation of actin-rich structures, including lamellipodia and dorsal membrane ruffles (6,7), invadopodia (8), podosomes (9), growth cones (10-12), and phagocytic cups (13,14). Three dynamin isoforms exist, namely, dynamin 1, 2, and 3 (5). Dynamins are characterized by a GTPase domain at the N-terminus, a bundle signaling element, a stalk domain, a phosphoinositide-binding pleckstrin homology domain, and a proline and arginine-rich domain at the C-terminus (PRD) (15,16). The PRD interacts with different proteins that contain the Src-homology-3 (SH3) domain. Of these GTPases, dynamin 2 is ubiquitously expressed.

Cortactin, an F-actin-binding protein, was first identified as an Src substrate (17). Cortactin also participates in cancer cell migration, invasion, and metastasis by regulating actin dynamics at the leading edge of migrating cells (18). Cortactin is composed of an N-terminal acidic domain and a six-and-a-half tandem repeats domain, which directly binds to F-actin. Cortactin also contains an α -helix, a proline-rich region, and an SH3 domain at the C-terminus, which interacts with the PRD of several binding partners (19).

Both dynamin and cortactin are implicated in the dynamics of cancer cells, including migration, invasion, and metastasis (18). In addition, the pharmacological inhibition of dynamin by GTPase inhibitors suppresses specific cellular processes such as the lamellipodial formation and invasion of human osteocarcinoma cells (20) and the growth of human prostate adenocarcinoma cells (21).

Correspondence to: Dr Hiroshi Yamada, Department of Neuroscience, Graduate School of Medicine, Dentistry and Pharmaceutical Sciences, Okayama University, 2-5-1 Shikata-cho, Kita-ku, Okayama 700-8558, Japan
E-mail: hiroyama@md.okayama-u.ac.jp

Key words: actin, cortactin, dynamin, filopodia, migration

A previous study reported that dynamin 2 binds to cortactin (7,12). A disruption of this protein complex can affect the shape of cancer cells (7), organization of the F-actin network within these cells (22), and structure of growth cones (11,12). However, the role of the dynamin 2-cortactin complex in the dynamics of the actin cytoskeleton in cancer cells is unclear. In this study, we investigated whether dynamin 2 and cortactin regulate the F-actin bundle formation in filopodia in the human non-small cell lung carcinoma cell line H1299.

Materials and methods

Antibodies and reagents. Rabbit polyclonal anti-dynamin 1 (cat. no. PA1-660; Thermo Fisher Scientific, Waltham, MA, USA) and anti-c-myc (cat. no. C3956; Sigma-Aldrich, St. Louis, MO, USA) antibodies, and a goat polyclonal anti-dynamin 2 (cat. no. sc-6400; Santa Cruz Biotechnology, Santa Cruz, CA, USA) antibody, were purchased. In addition, mouse monoclonal anti- β -actin (cat. no. A5441, Sigma-Aldrich), Dynasore (cat. no. D7693, Sigma-Aldrich), anti-c-myc (cat. no. sc-40; Santa Cruz Biotechnology), anti-green fluorescent protein (GFP; cat. no. sc-9996, Santa Cruz Biotechnology), and anti-cortactin (cat. no. 05-180; EMD Millipore, Darmstadt, Germany) antibodies were purchased. MitMAB and Dynole 34-2 were purchased from Abcam Biochemicals (Bristol, UK). Alexa Fluor 488-conjugated anti-rabbit IgG, rhodamine-conjugated anti-mouse IgG, and rhodamine or Alexa Fluor 488-labeled phalloidin were obtained from Thermo Fisher Scientific. Purified rabbit skeletal α -actinin was purchased from Cytoskeleton, Inc. (Denver, CO, USA). Goat anti-mouse IgG- and goat anti-rabbit IgG-conjugated gold particles were purchased from British BioCell International (Cardiff, UK).

Cell culture. The human non-small cell lung carcinoma cell line H1299 (Cat. no. ATCC CRL-5803; American Type Culture Collection, Manassas, VA, USA) was cultured in Dulbecco's modified Eagle's medium (DMEM, Thermo Fisher Scientific) supplemented with 10% fetal bovine serum (FBS) at 37°C in an atmosphere of 5% CO₂.

Expression and purification of dynamin 2 and cortactin wild-types and mutants. GFP-tagged dynamin 2 cloned into pEGFP-N1 was a kind gift from Dr Mark McNiven (Mayo Clinic, Rochester, MN, USA) (6). His-tagged dynamin 2 produced with the Bac-to-Bac baculovirus expression system (Thermo Fisher Scientific) was a kind gift from Dr Hiroshi Handa (Tokyo Institute of Technology, Tokyo, Japan) (23). The dynamin solution was concentrated using a Centrplus YM50 (Thermo Fisher Scientific) and stored at -80°C. The protein suspension (2-5 mg/ml protein) was thawed at 37°C before use.

The cDNAs encoding full-length rat cortactin and its mutants were prepared by polymerase chain reaction amplification using specific primers (12). Full-length cortactin or 1-450aa (Cort Δ SH3) was subcloned into the plasmid pGEX-6p vector as *Bam*HI-*Eco*RI fragments. GST-tagged cortactin W525K was generated by mutating pGEX-6p-cortactin with the QuickChange site-directed mutagenesis kit (Agilent Technologies, Santa Clara, CA, USA). For expression in cells, full-length cortactin or Cort Δ SH3 was subcloned into the pEF1 myc-His vector (Thermo Fisher Scientific) as *Eco*RI-*Xba*I

fragments. The nucleotide sequences of the constructs were verified by DNA sequence analysis. The resulting plasmid was transformed into the bacterial BL21 (DE3) pLysS strain for protein expression. The expression of GST-fusion proteins was induced by 0.1 mM isopropyl-1-thio-D-galactopyranoside at 37°C for 3-6 h in LB medium supplemented with 100 μ g/ml ampicillin to A₆₀₀ = 0.8. The purification of GST-fusion proteins was performed as previously described (24), and the cleavage of the GST with PreScission protease was performed according to the manufacturer's instructions. The protein was purified on a MonoQ column equilibrated in 20 mM Tris-HCl and 0.2 M NaCl, pH 7.7. The eluted protein fraction (1 mg/ml protein) was stored at -80°C. For the pull-down assay, the proteins were used without cleaving GST.

siRNA-mediated interference. Pre-annealed siRNAs for human dynamin 2 and cortactin, and the negative control siRNA, were synthesized and purified (Thermo Fisher Scientific). The sequences for the siRNAs for human dynamin 2 were as follows: 5'-GGAUUUUGAGGGCAAGAAGtt-3' (sense), 5'-CUUCUUGCCCUCAAUAUCCtt-3' (antisense) for oligo 1; 5'-GCGAAUCGUCACCACUUACtt-3' (sense), 5'-GUAAGUGGUGACGAUUCGtc-3' (antisense) for oligo 2; and 5'-GGACUUACGACGGGAGAUCtt-3' (sense), 5'-GAUCUCCCGU CGUAAGUCCtt-3' (antisense) for oligo 3. The sequences for the siRNAs for human cortactin were as follows: CCGAAUG GAUAAGUCAGUCtt-3' (sense), 5'-AGCUGACUUAUCCAU UCGGtc-3' (antisense) for oligo 1; GGUUUCGGCGGCA AAUACGtt-3' (sense), CGUAUUUGCCGCCGAAACtt-3' (antisense) for oligo 2; and CGAAUAUCAGUCGAAACUUtt-3' (sense), AAGUUUCGACUGAUUAUCGtg-3' (antisense) for oligo 3.

A scrambled siRNA with no significant sequence homology to all mouse, rat, or human gene sequences was used as the negative control. The day before transfection, the cells were plated in 6-well plates (5x10⁴ cells/well). One hundred picomoles of the duplex siRNAs was transfected into the cells using 4 μ l of Lipofectamine 2000 (Thermo Fisher Scientific). After 72 h, the cells were treated differently according to experimental design. In pilot experiments, we confirmed that all three transfections of siRNA for dynamin 2 and cortactin were effective.

Filopodial formation. H1299 cells were serum-starved for 16 h. Thereafter, the cells were transfected with dynamin 2 siRNAs, cortactin siRNAs, or the control siRNA, followed by incubation with DMEM supplemented with 10% FBS for 45 min. For the rescue experiments, cortactin was silenced in H1299 cells with oligo 3, and the cells were cultured for 24 h. The cells (1x10⁵/coverslip) were then transfected with rat wild-type cortactin or cortactin W525K (0.25 μ g each) cloned into the pIRES2-AcGFP1 expression vector (Clontech Laboratories, Santa Clara, CA, USA). Thereafter, the cells were stimulated with serum for 45 min, fixed, and stained with Alexa Fluor 488 or rhodamine-labeled phalloidin for visualization of filopodia.

Wound healing assay. H1299 cells were cultured to confluence on glass-bottom dishes (35 mm diameter; AGC Techno Glass Co. Ltd., Tokyo, Japan) in DMEM supplemented with 0.2% FBS

for 8 h. Thereafter, the cell layer was wounded with a plastic pipette tip as previously described (25). The cells were washed with DMEM supplemented with 0.2% FBS and incubated for 8 h in the presence of Dynasore, Dynole 34-2 or MitMAB at the indicated concentrations. For the negative control, cells were incubated with 1% dimethyl sulfoxide (DMSO). The cells were visualized by Giemsa staining, followed by the acquisition of phase contrast images from ≥ 20 randomly selected areas per dish. Areas filled with migrating cells were analyzed with ImageJ software (National Institutes of Health, Bethesda, MD, USA).

Formation of in vitro F-actin bundles. For the fluorescent detection of F-actin, non-muscle actin was polymerized in F-buffer (10 mM Tris-HCl, 0.2 mM DTT, 0.2 mM CaCl₂, 2 mM MgCl₂, 50 mM KCl, and 0.5 mM ATP, pH 7.5) for 1 h. Thereafter, 3.3 μ M F-actin was incubated with 5 μ M dynamin 1 or 2 and cortactin for 1 h, followed by an additional 30 min with 3 μ M Alexa Fluor 488-phalloidin. The samples were spread onto glass slides and mounted, and the F-actin bundles were observed under an epifluorescent microscope.

For the immunolocalization of dynamin and cortactin, F-actin bundles were incubated with dynamin 1 or 2 and cortactin for 30 min with 3 μ M phalloidin to stabilize the filaments, followed by centrifugation at 5,000 x g for 10 min. The pellet was resuspended with 50 μ l of F-buffer and then immunostained in suspension for 30 min with 1 μ l of primary antibody. The mixture was centrifuged at 5,000 x g, and the pellet was washed with F-buffer. The samples were incubated with secondary antibodies and washed as previously done for the primary antibody. All steps were performed at room temperature. The samples were spread onto glass slides and mounted. The samples were examined under a spinning disc confocal microscope system (CSU10, Yokogawa Electric Co., Tokyo, Japan) combined with an inverted microscope (IX-71, Olympus Optical Co., Ltd., Tokyo, Japan) and a CoolSNAP-HQ camera (Roper Technologies, Sarasota, FL, USA). The confocal system was controlled by MetaMorph software (Molecular Devices, Sunnyvale, CA, USA). Images were processed using Adobe Photoshop CS3 or Illustrator CS3 software.

Immunoprecipitation assay. For the immunoprecipitation assay, H1299 cells were co-transfected with GFP-tagged dynamin 2 and either myc-tagged cortactin or cortactin Δ SH3. The cells were lysed with 1% NP-40, 100 mM KCl, 0.5 mM EDTA, 10 mM NaF, and 20 mM HEPES/KOH, pH 7.4, and a protease inhibitor cocktail tablet (Roche Diagnostics, Basel, Switzerland). The protein complexes were immunoprecipitated from 1 mg of cell extract using either 5 μ g of the polyclonal anti-myc antibodies or preimmune IgG, and then visualized by western blotting with a monoclonal anti-GFP or anti-myc antibody.

Immunostaining and fluorescent microscopy. H1299 cells were fixed with 4% paraformaldehyde and stained by immunofluorescence as previously described (12).

Transmission electron microscopy. Specimens were embedded for immunoelectron microscopy as previously described (12). In

brief, H1299 cells were fixed with cytoskeleton buffer (10 mM 2-(N-morpholino)ethanesulfonic acid, 150 mM NaCl, 5 mM EGTA, 5 mM MgCl₂, and 5 mM glucose, pH 6.0) containing 10 μ g/ml phalloidin, 0.1% Triton X-100, and 3% formaldehyde for 1 min. The cells were then fixed for an additional 30 min without Triton X-100, followed by washing with 5 μ g/ml phalloidin in phosphate-buffered saline (PBS). After incubation in blocking solution (10 μ g/ml phalloidin, 2 mg/ml BSA, and 100 mM glycine in PBS), the specimens were incubated with a primary antibody diluted in blocking solution, washed with 5 μ g/ml phalloidin in PBS, incubated with goat anti-mouse or rabbit anti-goat IgG conjugated to 10-nm gold particles, and then fixed with 2.5% glutaraldehyde and 5 μ g/ml phalloidin in PBS. The specimens were post-fixed with 1% OsO₄ in 0.1 M sodium cacodylate buffer for 1 h, dehydrated, and embedded in EPON 812 for ultrathin sectioning. Cross-sections were visualized under a Hitachi H-7100 transmission electron microscope.

Determination of filopodial length. For the measurement of the filopodial length, H1299 cells were fixed and stained with rhodamine- or Alexa Fluor 488-conjugated phalloidin. Membrane protrusions supported with F-actin bundles were defined as filopodia, and digital images were acquired at 400-1,000x magnifications. Up to five filopodia for each cell were randomly selected, and their lengths were measured with ImageJ software.

Statistical analysis. Data were analyzed for statistical significance using KaleidaGraph software (version 4.1) for the Macintosh (Synergy Software Inc., Essex Junction, VT, USA). Analysis of variance and Tukey's honest significant difference post hoc test were applied for more than two different groups, and Student's t-test was applied for two different groups. P-values of <0.05 and 0.001 were considered as statistically significant.

Results

Inhibition of dynamin decreases the migration of the human non-small cell lung carcinoma cell line H1299. To determine whether dynamin 2 is involved in cell migration, the effects of dynamin inhibition on cell migration were determined by a wound healing assay. Cell migration decreased after treatment of cells with Dynasore (26), Dynole 34-2 (27), and MitMAB (28) (Fig. 1A). Dynasore (80 μ M) inhibited cell migration by ~80% compared to that of control cells, whereas Dynole 34-2 and MitMAB inhibited cell migration by 20-40% (Fig. 1B). These results indicate that dynamin is important for the migration of H1299 cells.

Dynamin 2 colocalizes with cortactin along F-actin bundles in filopodia of H1299 cells. Fig. 1 shows that dynamin is involved in cell migration mediated by pseudopodia. Thus, we investigated whether dynamin 2 participates in filopodial formation in H1299 cells. Because cortactin functions with dynamin 1 in the bundling of F-actin, which is important for the stability of filopodia in human neuroblastoma cell line SH-SY5Y (12), dynamin 2 and cortactin were immunostained in serum-stimulated H1299 cells. H1299 cells formed numerous filopodia

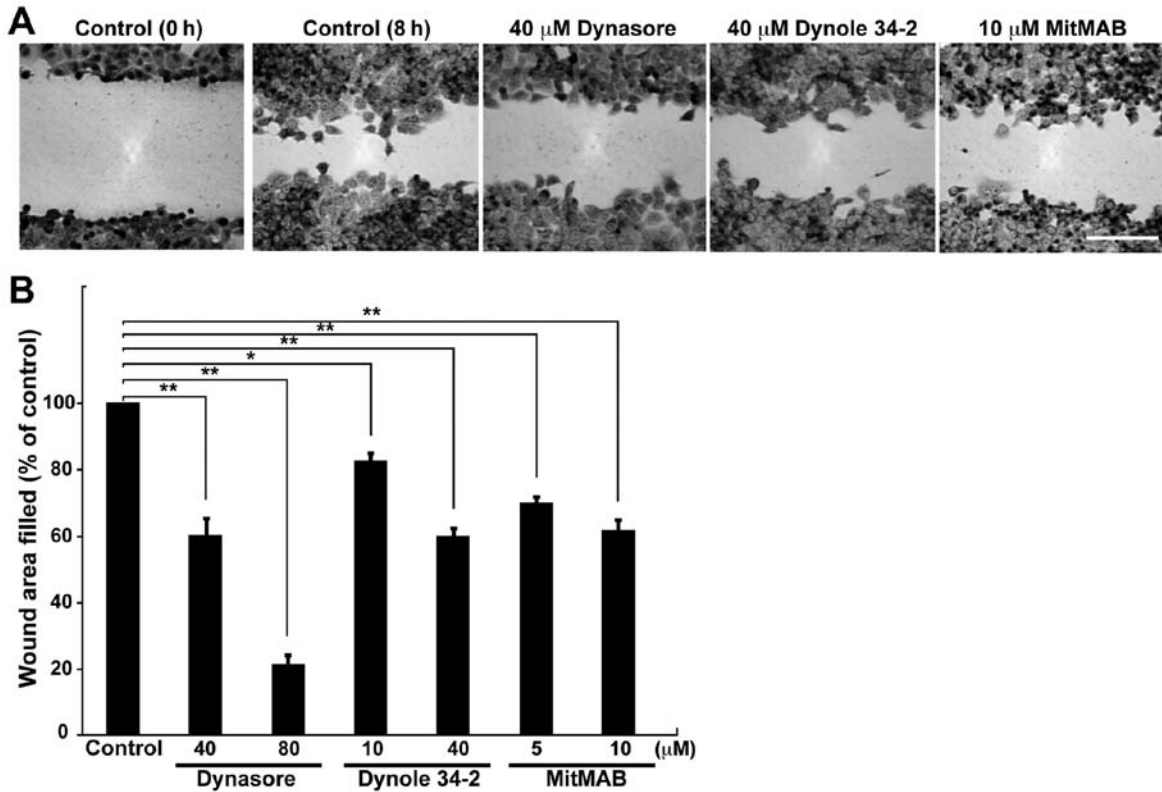


Figure 1. Dynamin GTPase inhibitors inhibit the migration of H1299 cells. (A) Representative images acquired by light microscopy showing cell migration in a wound healing assay. Confluent H1299 cells were wounded and then incubated for 8 h in the presence or absence of dynamin GTPase inhibitors at the indicated concentrations. For the negative control (control 0 h), cells were incubated with 1% DMSO. Scale bar, 200 μ m. (B) Morphometric analysis of the wound area filled by migrating cells after treatment with inhibitors at the indicated concentrations. The changes were normalized to the control. Results represent the means \pm SEM of three independent experiments.

after serum stimulation (Fig. 2A). Furthermore, dynamin 2 and cortactin colocalized to F-actin bundles in filopodia as bright dots (Fig. 2A). The negative controls showed little immunoreactivity for dynamin 2 and cortactin (Fig. 2B). In addition, immunoelectron microscopy revealed that both proteins localized to F-actin bundles in filopodia (Fig. 2C).

These results prompted us to examine the possible interaction of dynamin 2 and cortactin by immunoprecipitation. Exogenously expressed dynamin 2-GFP was co-precipitated with full-length cortactin-myc using a polyclonal anti-myc antibodies and H1299 cell lysates (Fig. 2D, left). Cort Δ SH3-myc, a dynamin 2 binding deficient mutant that lacks its SH3 domain, was unable to precipitate dynamin 2 (Fig. 2D, right). Taken together, these results illustrate that these proteins interact at F-actin bundles in filopodia of H1299 cells.

Dynamin 2 and cortactin are required for serum-induced filopodial formation in H1299 cells. To examine the role of dynamin 2 in filopodial formation, dynamin 2 was silenced in H1299 cells by RNAi. Compared with the control, knockdown of dynamin 2 in H1299 cells with specific siRNAs reduced its level by \sim 95% as revealed by western blotting (Fig. 3A). Compared with the length of filopodia in serum-stimulated control cells (10.2 \pm 0.5 μ m), dynamin 2 knockdown decreased filopodial extension in silenced cells (4.7 \pm 0.6 μ m) (Fig. 3B and C). In addition, dynasore inhibited filopodial extension (2.4 \pm 0.08 μ m). This effect was rescued after the inhibitor was removed (8.1 \pm 2.4 μ m) (Fig. 3D and E).

We also examined the effects of cortactin knockdown by RNAi on filopodial formation. Compared with the control, knockdown of cortactin reduced its level by \sim 95% as revealed by western blotting (Fig. 4A). Compared with the length of filopodia in control cells (10.2 \pm 0.39 μ m), cortactin knockdown also decreased filopodial extension after serum-stimulation (5.6 \pm 0.17 μ m) (Fig. 4B and C). The inhibition of filopodial formation in cortactin-silenced cells was rescued by exogenous expression of wild-type cortactin (10.8 \pm 0.54 μ m) but not by cortactin W525K, a binding-defective mutant of dynamin 2 (29) (Fig. 4D and E). In addition, the punctate-like localization of dynamin 2 along F-actin bundles reappeared in wild-type cortactin expressing cells (Fig. 4F, right). These results indicate that dynamin 2 and cortactin are required for filopodial formation.

F-actin bundling by the dynamin 2-cortactin complex stabilizes F-actin. The effects of dynamin 2 and cortactin on the formation of F-actin bundles were examined *in vitro*. In this experiment, preformed F-actin were incubated with or without cortactin and dynamin 2 in the presence of GTP. F-actin alone appeared as uniform filaments (Fig. 5A, actin alone). The addition of dynamin 2 to F-actin filaments did not cause any visible change in their distribution (Fig. 5A, + Dyn2). However, F-actin incubated with wild-type cortactin, cortactin W525K or cortactin Δ SH3 often formed small clusters (Fig. 5A, + Cort WT, + Cort W525K, or + Cort Δ SH3), consistent with a previously published report (12). The presence of both dynamin 2

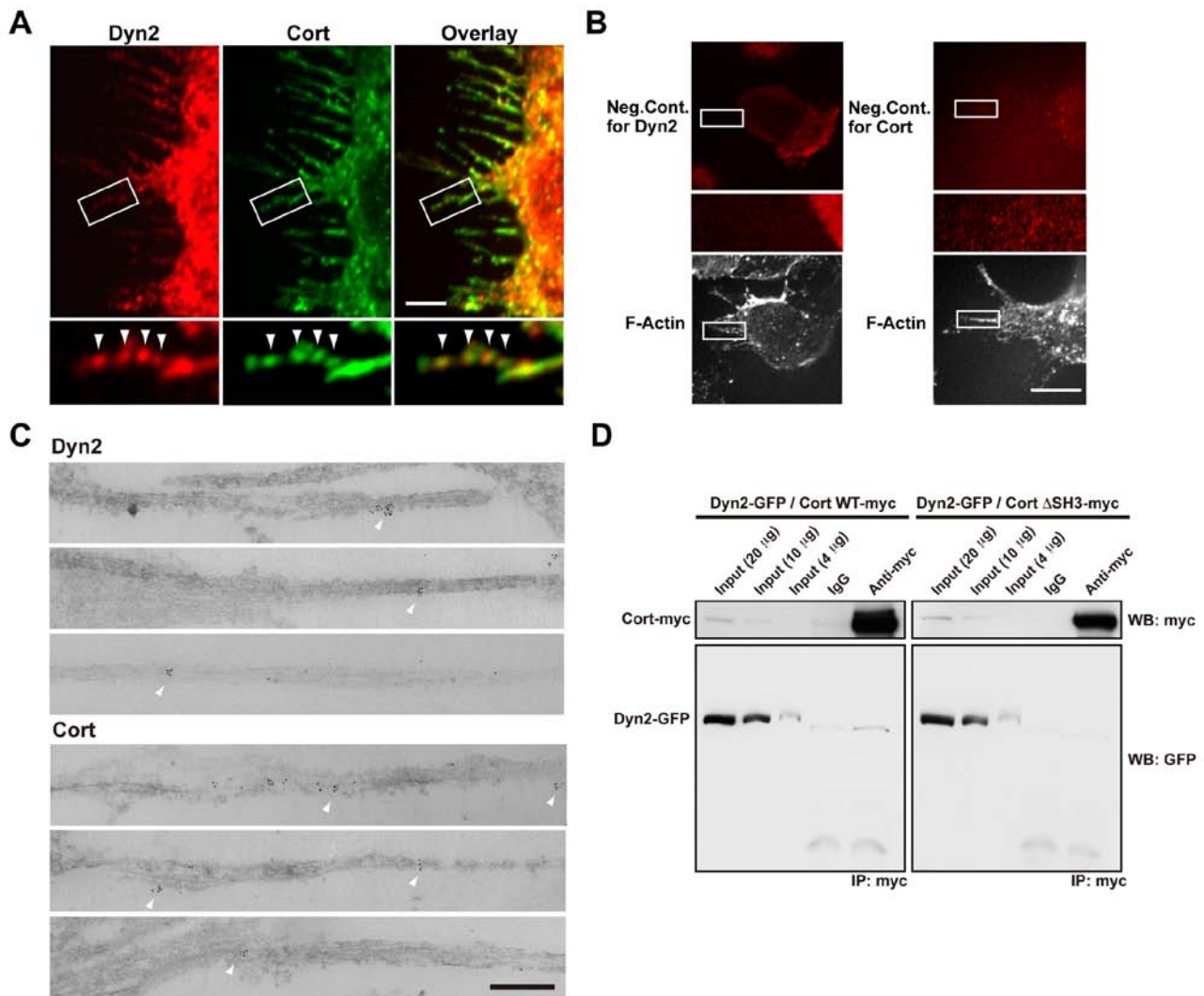


Figure 2. Dynamin 2 colocalizes with cortactin along F-actin bundles in filopodia of serum-stimulated H1299 cells. (A) Colocalization of dynamin 2 (Dyn2, left) and cortactin (Cort, middle) by double-immunofluorescent staining in filopodia of serum-stimulated H1299 cells. Boxed areas correspond to enlarged images shown below. Dynamin 2- and cortactin-positive puncta were present periodically along F-actin bundles in filopodia (arrowheads). Scale bar, 5 μm (upper panels), 1.6 μm (lower panels). (B) In the negative controls, the primary antibodies were omitted for dynamin 2 (left) and cortactin (right). Boxed areas correspond to enlarged images shown below. Bar, 10 μm (top and bottom panels), 2.8 μm (middle panels). (C) Representative images acquired by immunoelectron microscopy showing the localization of dynamin 2 (top three panels) and cortactin (bottom three panels) in filopodia of serum-stimulated H1299 cells. Immunoreactive dynamin 2 and cortactin were present along F-actin bundles (arrowheads). Scale bar, 20 nm. (D) Immunoprecipitation (IP) results demonstrating an *in vivo* interaction between dynamin 2 and cortactin. H1299 cells were co-transfected with GFP-tagged dynamin 2 (Dyn2-GFP) and either myc-tagged wild-type cortactin (Cort WT-myc, left) or cortactin ΔSH3 (Cort ΔSH3 -myc, right). The protein complexes were immunoprecipitated using a polyclonal anti-myc antibody or preimmune IgG (IgG), and then visualized by western blotting (WB) with monoclonal anti-GFP or anti-myc antibodies. Total cell lysates (4, 10 and 20 μg) were also analyzed (input).

and wild-type cortactin resulted in the formation of long and thick F-actin bundles (Fig. 5A, + Dyn2 + Cort WT), which were similar to those formed by dynamin 1 and cortactin (Fig. 5A, + Dyn1 + Cort WT). On the other hand, the long and thick F-actin bundles were much less evident in the presence of dynamin 2 and cortactin W525K or ΔSH3 (Fig. 5A, + Dyn2 + Cort W525K or + Dyn2 + Cort ΔSH3).

To localize dynamin 2 and cortactin to F-actin bundles, the preformed F-actin bundles were used for immunofluorescent staining. Dynamin 2 and cortactin colocalized as bright dots along F-actin bundles (Fig. 5B, left). The localization of dynamin 2 and cortactin was similar to that of the dynamin 1-cortactin complex (Fig. 5B, right) (12).

Lastly, we examined whether actin bundling by the dynamin 2-cortactin complex can affect F-actin stability.

To address this, the depolymerization kinetics of preformed pyrene-labeled F-actin were examined after the solution was diluted 10-fold with buffer. In the presence of dynamin 2 and cortactin, the rate of depolymerization by dilution decreased to a level comparable to that induced by α -actinin, an actin-crosslinking protein, indicating that dynamin 2 and cortactin stabilize F-actin bundles (Fig. 5C). These results indicate that the dynamin 2-cortactin complex stabilizes F-actin bundles in filopodia prior to cell migration.

Discussion

The involvement of dynamin in the dynamics of cancer cells such as cell migration, invasion, and metastasis has been reported (18). However, the precise role of dynamin in these

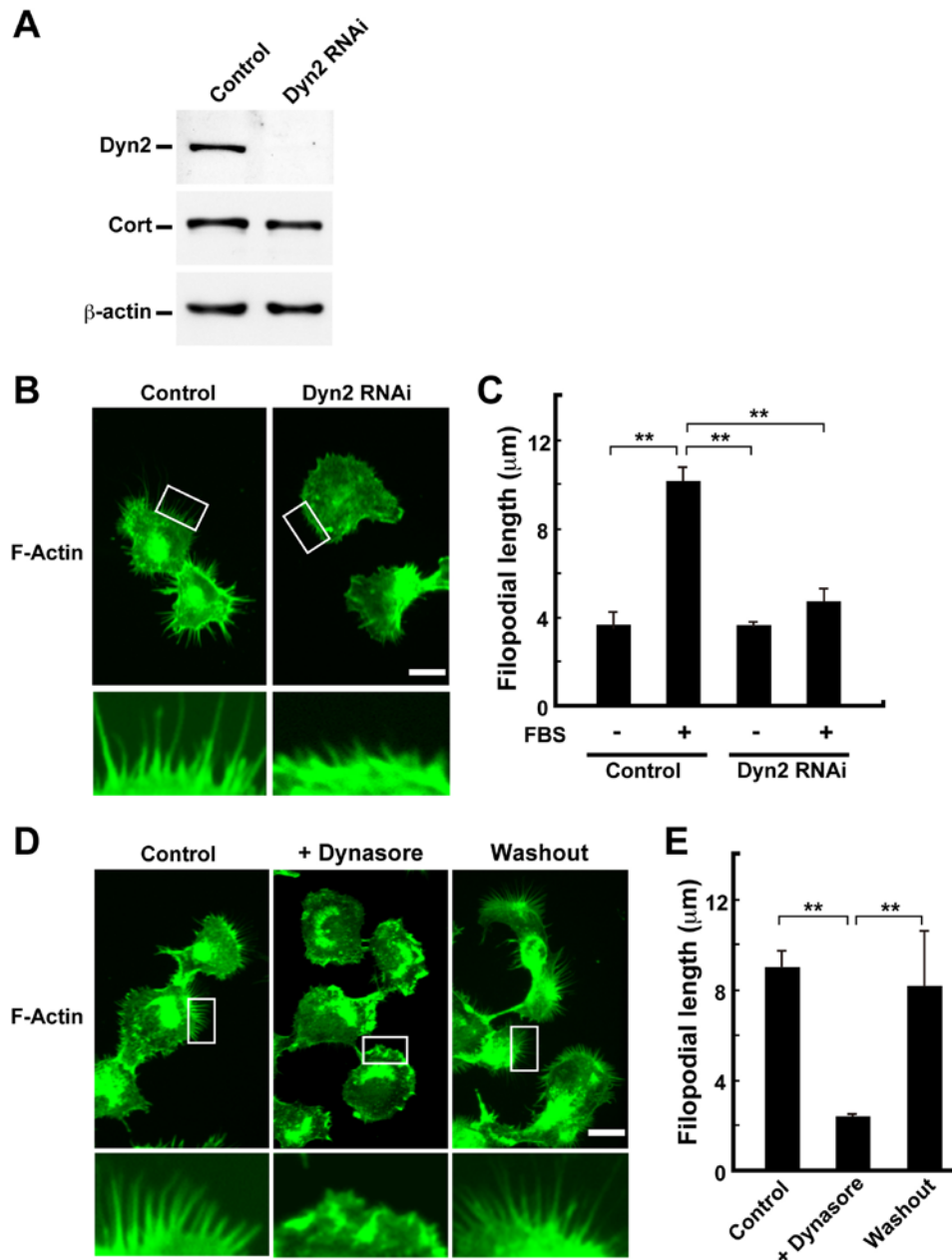


Figure 3. Knockdown of dynamin 2 decreases filopodial formation in H1299 cells. (A) Western blotting showing knockdown of dynamin 2 (Dyn2) expression by RNAi in H1299 cells. β -actin served as the control. Three micrograms of cell lysate from each sample was analyzed by gel electrophoresis. (B) F-actin was visualized in H1299 cells by Alexa Fluor 488-phalloidin staining after knockdown of dynamin 2. Extensive filopodial formation was observed in cells after serum stimulation (left). Filopodial formation was inhibited in dynamin 2-silenced cells (right). Boxed areas correspond to enlarged images shown below. Scale bar, 20 μ m (upper panels), 5 μ m (lower panels). (C) Filopodial length in H1299 cells cultured in the presence or absence of serum. The cells were visualized by fluorescent confocal microscopy, and filopodial length was measured as described in Materials and methods. (D) Inhibition of filopodial formation by dynasore in serum-stimulated H1299 cells. Serum-starved cells were incubated with 240 μ M dynasore for 30 min, and then stimulated with 10% FBS for 45 min in the presence of 240 μ M dynasore (middle). Thereafter, dynasore was removed, and the cells were incubated in serum-containing medium for 45 min (right). For the negative control, cells were cultured in the presence of 3% DMSO (left). All steps were performed at 37°C. (E) Analysis of filopodial formation in the H1299 cells shown in (D). The cells were analyzed by fluorescent confocal microscopy, and filopodial length was measured. Results in (C) and (E) represent the means \pm SEM from three independent experiments.

cellular processes is not entirely clear. We recently reported that actin bundling by the dynamin 1-cortactin complex is crucial for neurite extension in developing neurons (12). In this study, we examined the possibility that a similar F-actin-bundling mechanism is involved in the migration of H1299 cells, a human non-small cell lung carcinoma cell line.

We showed that cortactin and dynamin 2 mostly colocalized along F-actin bundles in filopodia of serum-stimulated

H1299 cells (Fig. 2). Pharmacological inhibition of dynamin 2 by Dynasore, Dynole 34-2 or MitMAB decreased cell migration (Fig. 1) and filopodial formation (Fig. 3). Furthermore, filopodia were shorter in dynamin 2- and cortactin-depleted cells than in control cells (Figs. 3 and 4). In cortactin-silenced cells, the exogenous expression of wild-type cortactin rescued the punctate-like localization of dynamin 2 and filopodial formation (Fig. 4). Both dynamin 2 and cortactin bundled

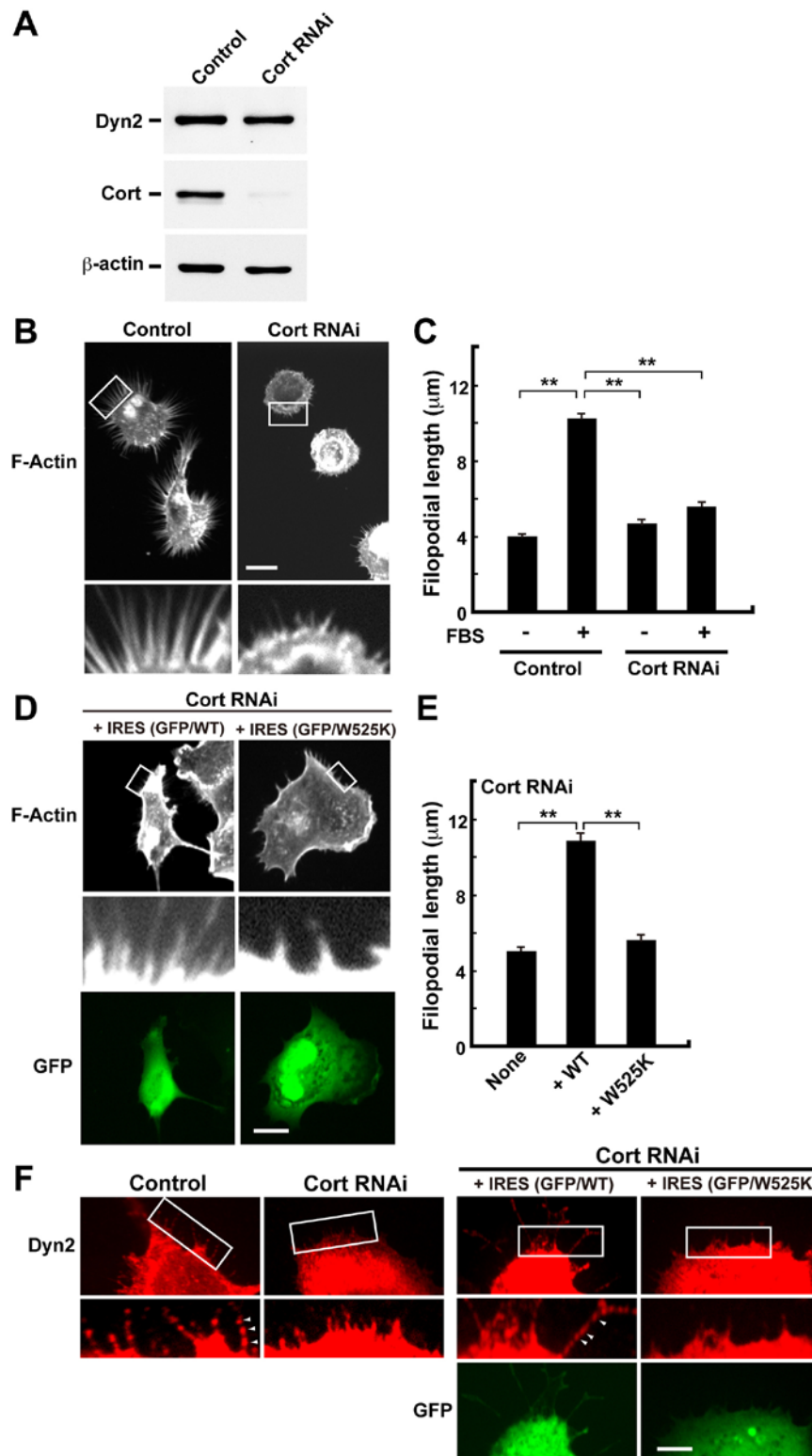


Figure 4. Knockdown of cortactin decreases filopodial formation in H1299 cells. (A) Western blotting showing knockdown of cortactin expression by RNAi in H1299 cells. β -actin was used as the control. Three micrograms of cell lysate from each sample was analyzed by gel electrophoresis. (B) F-actin was visualized in serum-stimulated H1299 cells by Alexa Fluor 488-phalloidin staining. Boxed areas correspond to enlarged images shown below. Similar to results from dynamin 2-depleted cells, filopodial formation decreased in cortactin-depleted cells (right). Scale bar, 20 μ m (upper panels), 5 μ m (lower panels). (C) Analysis of filopodial formation in H1299 cells cultured with or without serum. The samples were analyzed by fluorescent confocal microscopy, and the filopodial length was measured. (D) Expression of wild-type cortactin rescues filopodial formation. Cortactin-depleted H1299 cells were transfected with rat wild-type cortactin (left) or cortactin W525K (right) cloned into the pIRES2-AcGFP1 expression vector. Boxed areas correspond to enlarged images shown (middle panels). Transfected cells were identified by GFP expression (bottom panels). Scale bar, 20 μ m (top and bottom panels), 3.5 μ m (middle panels). (E) Analysis of filopodial formation in H1299 cells. The samples were analyzed by fluorescent confocal microscopy, and the filopodial length was measured. Results in (C) and (E) represent the means \pm SEM from three independent experiments. (F) Rescue of the punctate-like localization of dynamin 2 along F-actin bundles in filopodia by re-expression of cortactin in cortactin-depleted cells. Cortactin-depleted H1299 cells (left panels) were transfected with rat wild-type cortactin or cortactin W525K cloned into the pIRES2-AcGFP1 expression vector (right panels). The cells were immunostained with an anti-dynamin 2 antibodies. Boxed areas correspond to enlarged images shown below. Transfected cells were identified by GFP expression (right bottom panels). Scale bar, 5 μ m (top and right bottom panels), 2.3 μ m (left bottom and right middle panels).

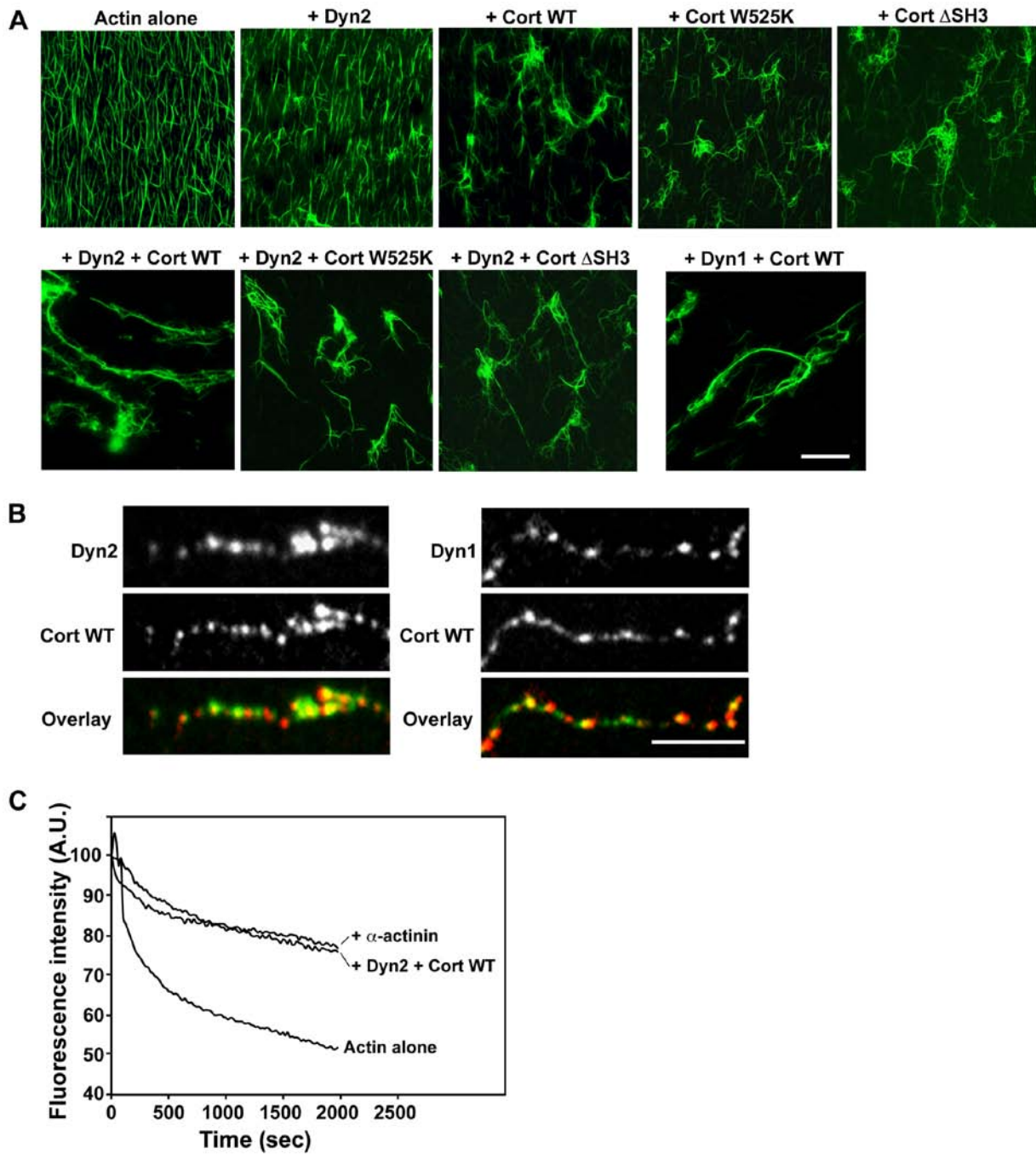


Figure 5. Actin bundling by dynamin 2 and cortactin stabilizes F-actin bundles. (A) Long F-actin bundles were formed in the presence of dynamin 2 and cortactin (lower left). Preformed F-actin ($3.3 \mu\text{M}$) was incubated with or without the indicated proteins ($5 \mu\text{M}$ each). F-actin was visualized with Alexa Fluor 488-phalloidin. Scale bar, $30 \mu\text{m}$. (B) Representative images acquired by fluorescent microscopy showing the localization of dynamin and cortactin along F-actin bundles. Actin bundles were formed *in vitro* by incubating dynamin 2 with wild-type cortactin (left) or dynamin 1 and wild-type cortactin (right). Protein colocalization was performed by double-immunofluorescence. Scale bar, $2 \mu\text{m}$. (C) Kinetics of F-actin disassembly induced in 10-fold diluted preformed pyrene-labeled F-actin solution with buffer. F-actin bundles disassembled in the presence of dynamin 2 and cortactin, as well as in the presence of $5 \mu\text{M}$ α -actinin. The rate of F-actin bundle disassembly was measured by pyrene-fluorescence.

F-actin, and these proteins increased F-actin stability (Fig. 5). These results indicate that dynamin 2 and cortactin participate in cancer cell migration by stabilizing F-actin bundles in filopodia.

Dynamin assembles at the neck of deeply invaginated endocytic pits (30). Upon GTP hydrolysis, however, dynamin undergoes a conformational change, resulting in the fission of endocytic pits and release of endocytic vesicles (31-33). In

addition, dynamin 1 forms a ring-like complex with cortactin, which switches from an open to a closed state upon GTP hydrolysis. This change promotes the bundling of F-actin filaments (12). The mechanism of actin bundling mediated by the dynamin 2-cortactin complex is similar to that of the dynamin 1-cortactin complex, because dynamin 2 and cortactin also facilitated the formation of long and thick F-actin bundles to which they colocalized (Fig. 5). This mechanochemical

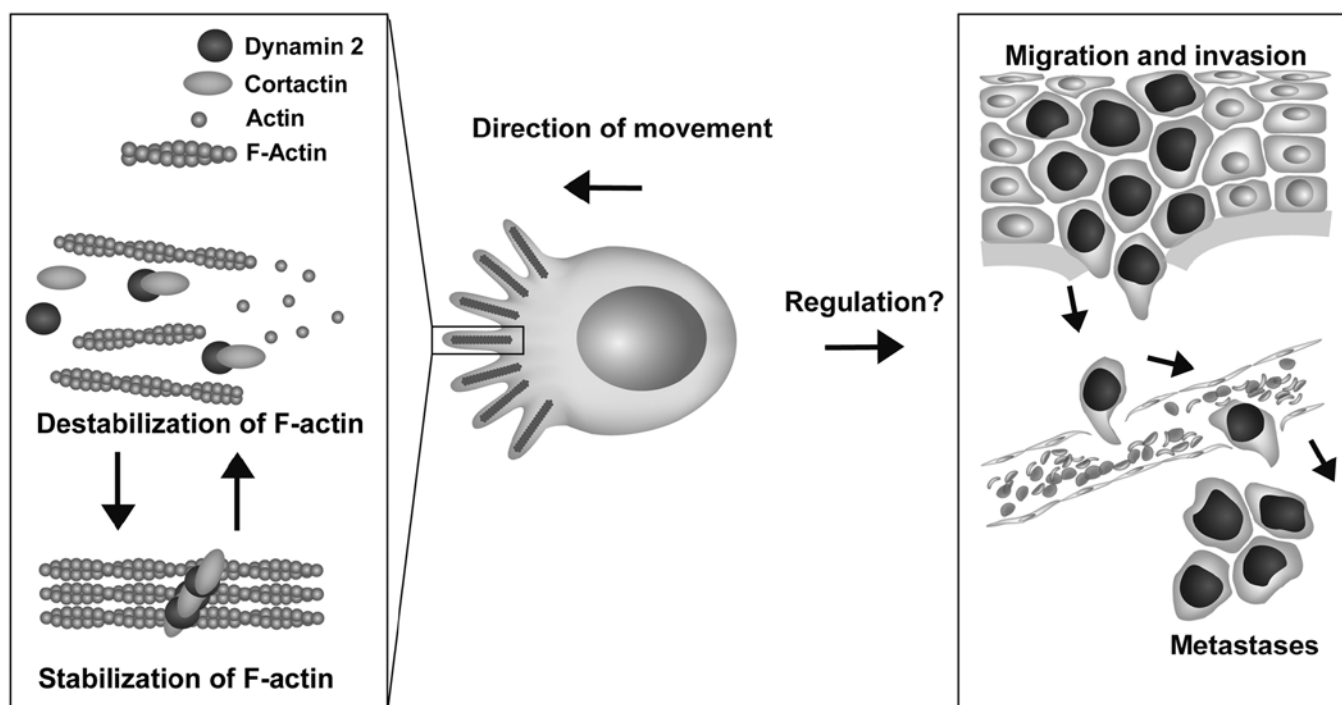


Figure 6. Putative role of the dynamin 2-cortactin complex in cancer cell migration. The dynamin 2-cortactin complex bundles actin filaments, which stabilize filopodia. In addition, the dynamin 2-cortactin complex participates in the formation of pseudopodia. The regulation of actin by dynamin 2 and cortactin may also be involved in cancer cell invasion and metastasis.

property may be critical for the formation of F-actin bundles in filopodia of other cell types as well (Fig. 6). Additional studies are needed to determine the precise mechanism.

Dynamamin associates with tumorigenesis, particularly tumor cell migration and invasion. For example, increased dynamamin 2 expression potentiates the migration and invasion of pancreatic ductal cancer cells (25), and tyrosine phosphorylated dynamamin 2 promotes the growth and invasiveness of glioblastomas (34). Thus, the involvement of dynamamin in the formation of F-actin bundles might promote cancer malignancy.

In conclusion, we showed that dynamamin 2 and cortactin participate in the formation of F-actin bundles, which stabilize filopodia in migrating cancer cells. Taken together, these results suggest that dynamamin might be a potential molecular target for anticancer therapy.

Acknowledgements

The authors thank Yuki Masuoka, Dr Shun-AI Li, and Nana Okazaki for technical assistance. This study was supported in part by grants from the Ministry of Education, Science, Sports, and Culture of Japan (grant no. 26670201 to H.Y.; grant no. 15K1533007 to K.T.), the Astellas Foundation for Research on Metabolic Disorders (to H.Y.), and the Japan Foundation for Applied Enzymology (to H.Y.).

References

- Arjonen A, Kaukonen R and Ivaska J: Filopodia and adhesion in cancer cell motility. *Cell Adhes Migr* 5: 421-430, 2011.
- Ridley AJ: Life at the leading edge. *Cell* 145: 1012-1022, 2011.
- Takei K, Slepnev VI, Haucke V and De Camilli P: Functional partnership between amphiphysin and dynamamin in clathrin-mediated endocytosis. *Nat Cell Biol* 1: 33-39, 1999.
- Mettlen M, Pucadyil T, Ramachandran R and Schmid SL: Dissecting dynamamin's role in clathrin-mediated endocytosis. *Biochem Soc Trans* 37: 1022-1026, 2009.
- Praefcke GJ and McMahon HT: The dynamamin superfamily: Universal membrane tubulation and fission molecules? *Nat Rev Mol Cell Biol* 5: 133-147, 2004.
- Cao H, Garcia F and McNiven MA: Differential distribution of dynamamin isoforms in mammalian cells. *Mol Biol Cell* 9: 2595-2609, 1998.
- McNiven MA, Kim L, Krueger EW, Orth JD, Cao H and Wong TW: Regulated interactions between dynamamin and the actin-binding protein cortactin modulate cell shape. *J Cell Biol* 151: 187-198, 2000.
- Baldassarre M, Pompeo A, Beznoussenko G, Castaldi C, Cortellino S, McNiven MA, Luini A and Buccione R: Dynamamin participates in focal extracellular matrix degradation by invasive cells. *Mol Biol Cell* 14: 1074-1084, 2003.
- Ochoa GC, Slepnev VI, Neff L, Ringstad N, Takei K, Daniell L, Kim W, Cao H, McNiven M, Baron R, *et al*: A functional link between dynamamin and the actin cytoskeleton at podosomes. *J Cell Biol* 150: 377-389, 2000.
- Torre E, McNiven MA and Urrutia R: Dynamamin 1 antisense oligonucleotide treatment prevents neurite formation in cultured hippocampal neurons. *J Biol Chem* 269: 32411-32417, 1994.
- Kurklinesky S, Chen J and McNiven MA: Growth cone morphology and spreading are regulated by a dynamamin-cortactin complex at point contacts in hippocampal neurons. *J Neurochem* 117: 48-60, 2011.
- Yamada H, Abe T, Satoh A, Okazaki N, Tago S, Kobayashi K, Yoshida Y, Oda Y, Watanabe M, Tomizawa K, *et al*: Stabilization of actin bundles by a dynamamin 1/cortactin ring complex is necessary for growth cone filopodia. *J Neurosci* 33: 4514-4526, 2013.
- Gold ES, Underhill DM, Morrisette NS, Guo J, McNiven MA and Aderem A: Dynamamin 2 is required for phagocytosis in macrophages. *J Exp Med* 190: 1849-1856, 1999.
- Otsuka A, Abe T, Watanabe M, Yagisawa H, Takei K and Yamada H: Dynamamin 2 is required for actin assembly in phagocytosis in Sertoli cells. *Biochem Biophys Res Commun* 378: 478-482, 2009.
- Faelber K, Posor Y, Gao S, Held M, Roske Y, Schulze D, Haucke V, Noé F and Daumke O: Crystal structure of nucleotide-free dynamamin. *Nature* 477: 556-560, 2011.

16. Ford MG, Jenni S and Nunnari J: The crystal structure of dynamin. *Nature* 477: 561-566, 2011.
17. Wu H, Reynolds AB, Kanner SB, Vines RR and Parsons JT: Identification and characterization of a novel cytoskeleton-associated pp60src substrate. *Mol Cell Biol* 11: 5113-5124, 1991.
18. MacGrath SM and Koleske AJ: Cortactin in cell migration and cancer at a glance. *J Cell Sci* 125: 1621-1626, 2012.
19. Ammer AG and Weed SA: Cortactin branches out: Roles in regulating protrusive actin dynamics. *Cell Motil Cytoskeleton* 65: 687-707, 2008.
20. Yamada H, Abe T, Li SA, Masuoka Y, Isoda M, Watanabe M, Nasu Y, Kumon H, Asai A and Takei K: Dynasore, a dynamin inhibitor, suppresses lamellipodia formation and cancer cell invasion by destabilizing actin filaments. *Biochem Biophys Res Commun* 390: 1142-1148, 2009.
21. Yamada H, Abe T, Li SA, Tago S, Huang P, Watanabe M, Ikeda S, Ogo N, Asai A and Takei K: N'-[4-(dipropylamino)benzylidene]-2-hydroxybenzohydrazide is a dynamin GTPase inhibitor that suppresses cancer cell migration and invasion by inhibiting actin polymerization. *Biochem Biophys Res Commun* 443: 511-517, 2014.
22. Mooren OL, Kotova TI, Moore AJ and Schafer DA: Dynamin2 GTPase and cortactin remodel actin filaments. *J Biol Chem* 284: 23995-24005, 2009.
23. Masaike Y, Takagi T, Hirota M, Yamada J, Ishihara S, Yung TM, Inoue T, Sawa C, Sagara H, Sakamoto S, *et al*: Identification of dynamin-2-mediated endocytosis as a new target of osteoporosis drugs, bisphosphonates. *Mol Pharmacol* 77: 262-269, 2010.
24. Slepnev VI, Ochoa GC, Butler MH and De Camilli P: Tandem arrangement of the clathrin and AP-2 binding domains in amphiphysin 1 and disruption of clathrin coat function by amphiphysin fragments comprising these sites. *J Biol Chem* 275: 17583-17589, 2000.
25. Eppinga RD, Krueger EW, Weller SG, Zhang L, Cao H and McNiven MA: Increased expression of the large GTPase dynamin 2 potentiates metastatic migration and invasion of pancreatic ductal carcinoma. *Oncogene* 31: 1228-1241, 2012.
26. Macia E, Ehrlich M, Massol R, Boucrot E, Brunner C and Kirchhausen T: Dynasore, a cell-permeable inhibitor of dynamin. *Dev Cell* 10: 839-850, 2006.
27. Hill TA, Gordon CP, McGeachie AB, Venn-Brown B, Odell LR, Chau N, Quan A, Mariana A, Sakoff JA, Chircop M, *et al*: Inhibition of dynamin mediated endocytosis by the dynoles-synthesis and functional activity of a family of indoles. *J Med Chem* 52: 3762-3773, 2009.
28. Quan A, McGeachie AB, Keating DJ, van Dam EM, Rusak J, Chau N, Malladi CS, Chen C, McCluskey A, Cousin MA, *et al*: Myristyl trimethyl ammonium bromide and octadecyl trimethyl ammonium bromide are surface-active small molecule dynamin inhibitors that block endocytosis mediated by dynamin I or dynamin II. *Mol Pharmacol* 72: 1425-1439, 2007.
29. Schafer DA, Weed SA, Binns D, Karginov AV, Parsons JT and Cooper JA: Dynamin 2 and cortactin regulate actin assembly and filament organization. *Curr Biol* 12: 1852-1857, 2002.
30. Takei K, McPherson PS, Schmid SL and De Camilli P: Tubular membrane invaginations coated by dynamin rings are induced by GTP-gamma S in nerve terminals. *Nature* 374: 186-190, 1995.
31. Sweitzer SM and Hinshaw JE: Dynamin undergoes a GTP-dependent conformational change causing vesiculation. *Cell* 93: 1021-1029, 1998.
32. Takei K, Haucke V, Slepnev V, Farsad K, Salazar M, Chen H and De Camilli P: Generation of coated intermediates of clathrin-mediated endocytosis on protein-free liposomes. *Cell* 94: 131-141, 1998.
33. Roux A, Uyhazi K, Frost A and De Camilli P: GTP-dependent twisting of dynamin implicates constriction and tension in membrane fission. *Nature* 441: 528-531, 2006.
34. Feng H, Liu KW, Guo P, Zhang P, Cheng T, McNiven MA, Johnson GR, Hu B and Cheng SY: Dynamin 2 mediates PDGFR α -SHP-2-promoted glioblastoma growth and invasion. *Oncogene* 31: 2691-2702, 2012.